Advances in Military Technology
Vol. 21, No. 1, 2026, pp. 247-261
ISSN 1802-2308, eISSN 2533-4123
DOI 10.3849/aimt.02011

Open Conceptual Design of a Multi-Mission Tactical Quadcopter Using COTS Components

R. Octavianty[1,2]*, F. S. Jahan[1], and T. Simanjuntak[1,2]

[1] *International University Liaison Indonesia, Tangerang, Indonesia*
[2] *Indonesia Euler Institute, South Tangerang, Indonesia*

The manuscript was received on 3 July 2025 and was accepted after revision for publication as a case study on 19 May 2026.

Abstract:

This paper presents an open conceptual design of a multi-mission tactical quadcopter addressing payload limitations in existing commercial loitering munitions. Using Components-Off-The-Shelf (COTS) components, the design achieves 400–600 g payload capacity – a 120 % increase over commercial alternatives – enabling compatibility with standard military ordnance such as the Indonesian GT5-PEA2 defensive grenade (430 g). The modular design supports three mission profiles: ISR, payload delivery, and kamikaze operations, with a foldable configuration stowing within 180 mm for infantry portability. The ISR configuration achieves 30 min endurance and 6 790 m range. Unit production cost of 774 USD represents a 68 % reduction versus commercial alternatives. Complete design documentation is publicly available to accelerate collaborative development.

Keywords:

loitering munition, COTS components, multi-mission UAV

1 Introduction

Contemporary military operations are increasingly characterized by urban combat scenarios, where dense infrastructure, vertical terrain, and high civilian population density create unique operational challenges demanding innovative technological solutions [1–4]. Urban warfare reduces typical engagement distances from kilometers to tens of meters while introducing complex vertical dimensions where adversaries exploit building structures for concealment and tactical advantage [5]. These conditions necessitate precision engagement capabilities that minimize collateral damage while

* *Corresponding author: Department of Aviation Engineering, International University Liaison Indonesia, Tangerang, Indonesia, 15332, Phone: +62 877-5426-9717, E-mail: ressa.octavianty@euler-institute.org. ORCID 0000-0001-5130-0298.*

maximizing operational effectiveness – requirements that traditional artillery and air support systems designed for open battlefield conditions often fail to meet.

Unmanned Aerial Vehicles (UAVs) have emerged as indispensable force multipliers for urban military operations, providing persistent intelligence, surveillance, and reconnaissance (ISR) while minimizing risk to personnel [6]. Recent conflicts have demonstrated their transformative impact, with loitering munitions proving particularly effective for precision engagement in urban terrain [7]. Among various UAV configurations, fixed-wing platforms represent 78 % of operational loitering munitions due to their superior range and endurance [8, 9]. However, their operational advantages diminish significantly in urban environments where hovering capability, vertical take-off and landing in confined spaces, and navigation through narrow building corridors become paramount. Multirotor platforms, particularly quadcopters, offer superior capabilities for these demanding requirements [6].

Tactical UAV employment in urban combat is further constrained by infantry load limitations. The U.S. Army Field Manual FM 21–18 establishes maximum load standards of 21.7 kg for combat operations [10], with biomechanical research confirming that exceeding these limits significantly increases musculoskeletal injury risk [11, 12]. These constraints necessitate strict adherence to weight and portability requirements in any tactical UAV design.

A critical capability gap exists in current commercial platforms regarding payload capacity. Market-available tactical quadcopters such as the SpearUAV Viper40 and Defendtex Drone40 are limited to 200 g payload or less [8] – incompatible with standard military ordnance such as the Indonesian GT5-PEA2 defensive grenade (430 g) [13]. Additionally, current commercial loitering munitions cost approximately 2 400 USD per unit, creating barriers to widespread infantry-level adoption.

This paper addresses these gaps through an open conceptual design of a multi-mission tactical quadcopter engineered to overcome existing payload and cost limitations. Three primary objectives guide the design: achieving (400–600) g payload capacity to accommodate standard military ordnance; maintaining compact dimensions for infantry portability; and utilizing COTS components to minimize cost and enable rapid deployment. The design supports three mission profiles as illustrated in Fig. 1: ISR, payload delivery, and kamikaze operations. The open design approach – with complete CAD files, specifications, and manufacturing guidelines made publicly available – democratizes access to advanced tactical UAV technology and facilitates collaborative development.

2 Design Requirements and Conceptual Sizing

2.1 Benchmarking Analysis

The initial sizing process began with a comprehensive benchmarking study of existing tactical quadcopter loitering munitions. Two representative commercial platforms were analyzed: the SpearUAV Viper40 and the Defendtex Drone40. These systems represent the current state-of-the-art in tactical multirotor loitering munitions and provide baseline performance metrics for the new design.

Tab. 1 presents the detailed specifications of both benchmark platforms. A critical limitation identified in both systems is the maximum payload capacity of ≤ 200 g, which is insufficient for standard military ordnance such as the Indonesian military's GT5-PEA2 defensive grenade (430 g). This payload constraint represents a significant operational gap that the proposed design aims to address.

Analysis of the benchmark data reveals an average payload ratio of $f_{\mathrm{pl}} = 0.535$, which serves as a baseline for the new design's mass allocation strategy.

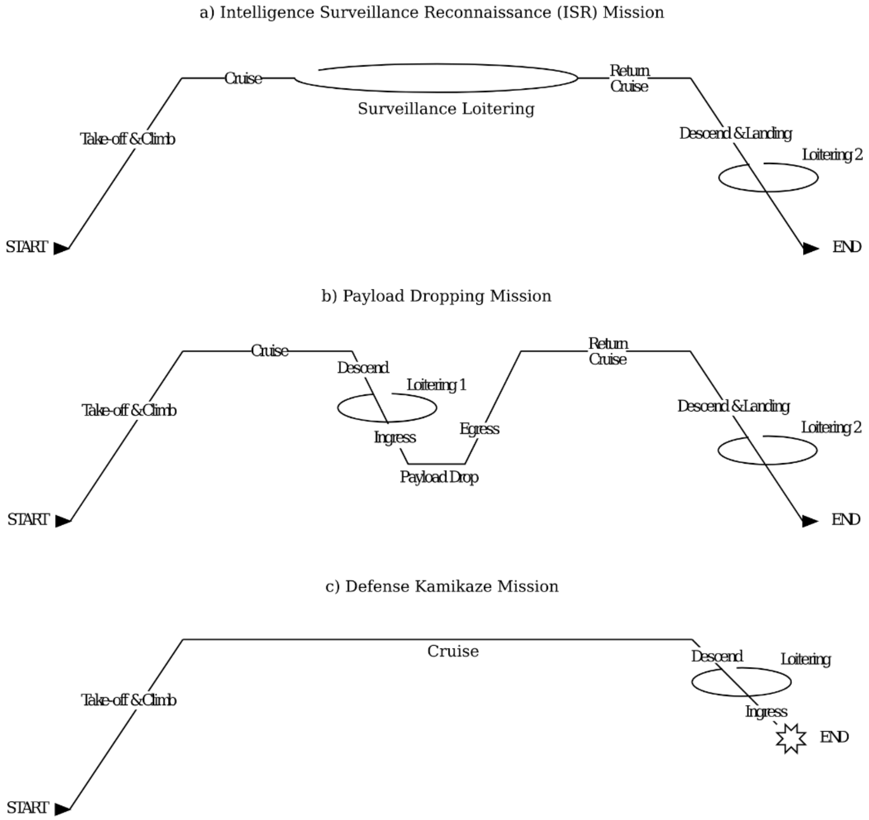

Fig. 1 Three operational mission profiles enabled by the multi-mission quadcopter design: (a) Intelligence, Surveillance, and Reconnaissance (ISR) for persistent area monitoring; (b) Payload delivery for precision ordnance deployment; and (c) Kamikaze operations for direct target engagement

Tab. 1 Benchmarking of commercial quadcopter loitering munitions

No.	Specification Parameters	Viper40	Drone40	Units
1	Maximum Take-Off Mass (MTOM)	450	300	g
2	Maximum Operating Empty Mass (MOEM)	250	110	g
3	Payload Mass (m_{pl})	200	190	g
4	Payload Ratio ($f_{\mathrm{pl}} = m_{\mathrm{pl}}$/MTOM)	0.44	0.63	—
5	Maximum Speed	18	20	m/s
6	Endurance at MTOM	25	30	min
7	Endurance at MOEM	35	60	min
8	Maximum Range at MTOM	1 000	20 000	m
9	Maximum Range at MOEM	5 000	20 000	m
10	Maximum Length (Folded)	—	180	mm
11	Diameter	40	40	mm

2.2 Design Requirements and Objectives

Based on the operational requirements for Indonesian military applications and the identified gaps in existing commercial platforms, the design requirements and objectives were established as presented in Tab. 2. The requirements are categorized into mandatory minimum specifications and aspirational goals to guide the design optimization process.

The primary design driver is the payload requirement of 400 g to 600 g, which necessitates a significant increase in MTOM compared to existing platforms. This requirement directly supports compatibility with standard military ordnance, particularly the GT5-PEA2 defensive grenade (430 g) used by Indonesian forces.

Tab. 2 Design requirements and objectives

No.	Design Requirements	Mandatory	Goal	Units
1	Maximum Payload	400	600	g
2	Endurance at MTOM	15	30	min
3	Endurance at MOEM	30	60	min
4	Range at MTOM	1 000	5 000	m
5	Range at MOEM	5 000	10 000	m
6	Maximum Speed	18	21	m/s

2.3 Initial Mass Estimation

The initial gross MTOM estimation was derived from the benchmark payload ratio analysis. Using the average payload ratio of $f_{\mathrm{pl}} = 0.535$ and targeting a 430 g payload (GT5-PEA2 grenade), the preliminary MTOM estimate was calculated as:

$$\mathrm{MTOM}_{\mathrm{initial}} = \frac{m_{\mathrm{payload}}}{f_{\mathrm{pl}}} = \frac{430\ \mathrm{g}}{0.535} = 804\ \mathrm{g} \tag{1}$$

Rounding up to account for design uncertainties and additional payload mounting hardware, an initial design MTOM of 850 g was established for subsequent propulsion system sizing.

2.4 Propulsion System Sizing

The total thrust requirement for the quadcopter was determined using a load factor approach. The load factor (l_{f}) represents the ratio between required thrust force and aircraft weight, providing adequate thrust margin for maneuvering and disturbance rejection. According to [14, 15], typical load factors for small quadcopters range from 2.0 to 2.5, with 2.3 being commonly used for tactical applications.

The total required thrust was calculated as:

$$F_{\mathrm{required}} = l_{\mathrm{f}} \cdot W \cdot g = 2.3 \cdot\ 0.85\ \mathrm{kg} \cdot 9.81\ \mathrm{ms}^{-2} = 19.1\ \mathrm{N} \tag{2}$$

Distributing this thrust equally among four propellers:

$$F_{\mathrm{per\ propeller}} = \frac{F_{\mathrm{required}}}{4} = \frac{19.1\ \mathrm{N}}{4} = 4.78\ \mathrm{N} \tag{3}$$

A 6 in (152.4 mm) diameter propeller with 3 in (76.2 mm) pitch was selected based on market availability and dimensional constraints for the folding configuration. The propeller performance characteristics were estimated using blade element theory, with thrust coefficient $C_T = 0.041$, torque coefficient $C_Q = 0.0036$, and design advance ratio $J = 0.375$.

To generate the required thrust of 4.78 N per propeller, the necessary rotational speed was calculated using the thrust equation:

$$T = \rho n^2 D^4 C_T \tag{4}$$

Solving for rotational speed:

$$n = \sqrt{\frac{T}{\rho D^4 C_T}} = \sqrt{\frac{4.78\ \text{N}}{1.225\ \text{kg}\,\text{m}^{-3} \cdot (0.152\ \text{m})^4 \cdot 0.041}} = 417\ \text{s}^{-1} \qquad \left(25\,020\ \text{min}^{-1}\right) \tag{5}$$

This rotational speed requirement guided the subsequent motor selection process, ensuring compatibility between propeller characteristics and motor performance capabilities. The calculated thrust-to-weight ratio of 2.3 provides adequate performance margins for hovering, maneuvering, and stability maintenance across all mission configurations [16].

3 System Design and Architecture

3.1 Overall System Architecture

The quadcopter employs a modular architecture enabling rapid reconfiguration between three mission profiles: ISR, payload delivery, and kamikaze operations, as illustrated in Fig. 1. The architecture prioritizes compactness, portability, and operational flexibility while maintaining structural integrity under tactical deployment conditions. Standardized interfaces and component exchanges enable mission reconfiguration, maximizing operational utility while minimizing logistical burden on infantry units.

The core design centers on a foldable configuration that minimizes storage volume for infantry transport while providing adequate performance when deployed. The folded configuration achieves maximum dimensions of 180 mm, facilitating integration with standard military equipment loadouts, as illustrated in Fig. 2. Complete CAD documentation is publicly available at [CAD Model – OnShape] to support collaborative development and manufacturing.

Each mission profile presents unique operational requirements and payload configurations. The ISR mission utilizes the quadcopter at minimum weight for maximum endurance and range, carrying only essential sensor equipment. The payload delivery mission incorporates the full grenade mounting system for precision ordnance deployment at designated targets. The kamikaze mission converts the entire platform into the delivery mechanism, representing the ultimate force multiplication capability.

3.2 Airframe Design and Materials Selection

The airframe employs a symmetric X-configuration with four foldable arms that rotate about central pivot points. This configuration provides several advantages: uniform load distribution across all four propulsion units, simplified flight control algorithms, and compact folding geometry. The unfolded configuration, shown in Fig. 3, achieves a rotor disk diameter of 400 mm with 6 in (152.4 mm) propellers.

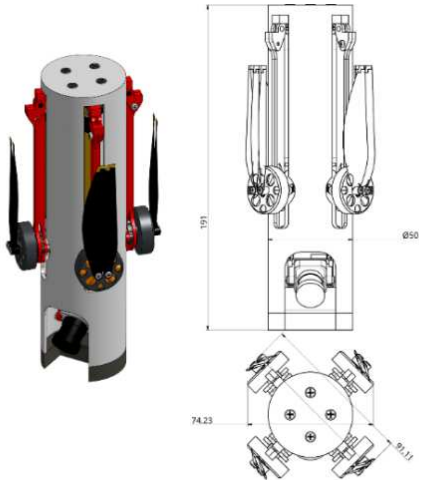

Fig. 2 Three-view drawing of quadcopter in folded configuration at maximum operating empty mass (MOEM). Dimensions shown in millimeters

Polycarbonate was selected as the primary structural material based on a comprehensive trade study considering strength-to-weight ratio, manufacturing feasibility, and cost constraints. Polycarbonate offers several critical advantages for tactical UAV applications: superior impact resistance compared to alternative polymers essential for tactical deployment scenarios, excellent 3D printing characteristics enabling rapid prototyping [17] and low-volume production, favorable density of 1.2 g/cm^3 providing optimal strength-to-weight ratio, resistance to temperature variations and UV degradation typical in field operations, and cost effectiveness through readily available material with established supply chains.

The total airframe mass of 109.0 g represents 12.8 % of the maximum take-off mass, indicating efficient structural design. Component thickness varies from 1.5 mm for non-load-bearing panels to 3.0 mm for critical structural joints and motor mounts.

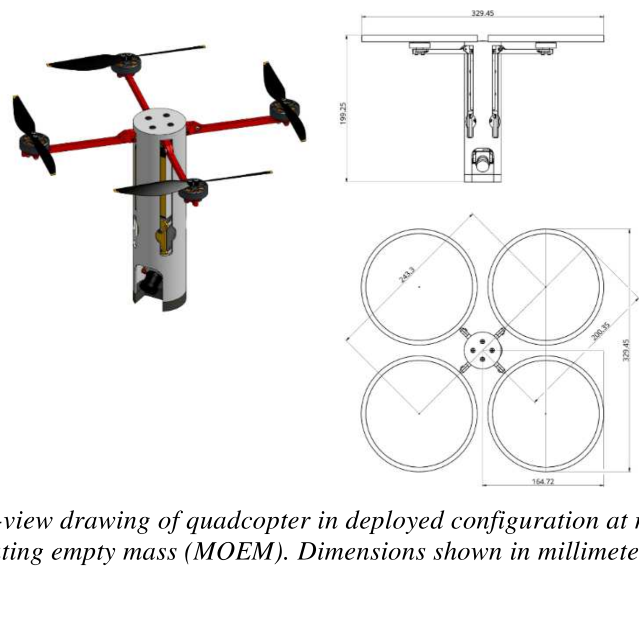

Fig. 3 Three-view drawing of quadcopter in deployed configuration at maximum operating empty mass (MOEM). Dimensions shown in millimeters

3.3 Component Integration and Layout

Fig. 4 illustrates the optimized component layout within the central fuselage. The arrangement prioritizes center-of-gravity control, thermal management, and accessibility for maintenance operations. The battery pack, representing the largest single mass component at 167.0 g, is positioned at the geometric center to minimize CG shift between mission configurations.

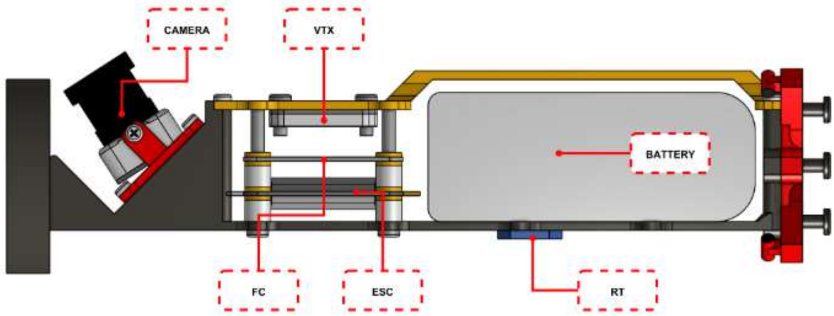

Fig. 4 Internal component arrangement showing optimized layout for center-of-gravity control and thermal management¨

The propulsion system consists of four brushless DC motors rated at 16.4 g each, selected to meet the rotational speed requirement of 25 020/min calculated in Section 2.4. The motors are mounted using vibration-isolating elastomeric bushings to minimize structural fatigue and improve flight stability. Each motor-propeller combination generates the required 4.78 N thrust at maximum power settings.

The avionics suite integrates commercial-off-the-shelf components optimized for weight and performance. The T-Motor F7 + F55A PRO II flight controller provides integrated flight control and electronic speed control functionality, while the Matek ELRS 2.4GHz receiver enables secure telemetry and control links. The video system comprises a RunCam Eagle 3 Night Vision camera with T-Motor FT800 video transmitter for real-time ISR capabilities. Power management utilizes a Tattu R-Line 1 550mAh 4S 130C battery pack optimized for high discharge rate applications.

3.4 Payload Mounting and Release System

The payload mounting system employs a modular approach that enables rapid reconfiguration between mission types. For payload delivery and kamikaze missions, the GT5-PEA2 defensive grenade (430 g, 50 mm diameter) mounts to the ventral surface via a custom interface shown in Fig. 5. The mounting system mass of 35.2 g includes all structural components, release mechanisms, and attachment hardware. The design accommodates center-of-gravity variations between loaded and unloaded configurations while maintaining flight stability margins.

Fig. 6 details the electromechanical release system designed for reliable payload deployment. The mechanism employs a fail-safe design philosophy where the default state secures the payload, and active servo actuation is required for release. The operating sequence follows four distinct phases: pre-flight preparation where the safety pin is removed and payload secured by safety lever and retention strap; in-flight operation where payload is held by mechanical retention system independent of electrical power; release command execution where servo motor actuates release hook, lifting aluminum retention rod; and payload separation where strap tension releases safety lever, initiating grenade fuse sequence.

The release mechanism incorporates multiple safety features to prevent inadvertent activation, including mechanical retention as primary safety system, electrical actuation required for release (fail-safe to secure), physical separation between release mechanism and grenade arming system, and manual safety pin for ground handling operations. This comprehensive safety approach ensures reliable operation under combat conditions while preventing accidental deployment during transport or handling.

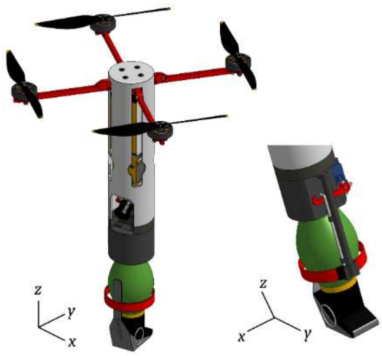

Fig. 4 Modular payload mounting system designed for GT5-PEA2 defensive grenade integration

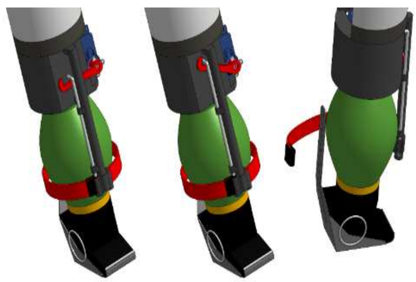

Fig. 5 Electromechanical payload release mechanism with fail-safe design architecture

3.5 Mission Configuration Analysis

The modular design enables 465.2 g mass reduction when transitioning from payload delivery to ISR configuration, as detailed in Tab. 3. This significant mass variation between mission profiles demonstrates the flexibility of the modular architecture while highlighting the performance trade-offs inherent in multi-mission design.

Tab. 3 Detailed mass breakdown by mission configuration

No.	Component	ISR [g]	Payload [g]	Kamikaze [g]
1	Airframe	109.0	109.0	109.0
2	Flight Controller	7.4	7.4	7.4
3	Electronic Speed Controller	17.5	17.5	17.5
4	Battery	167.0	167.0	167.0
5	Motors (4×)	65.6	65.6	65.6
6	Propellers (4×)	3.6	3.6	3.6
7	Video Transmitter	7.6	7.6	7.6
8	Radio Receiver	1.2	1.2	1.2
9	Camera	8.5	8.5	8.5
10	Payload Mounting Support	—	35.2	35.2
11	GT5-PEA2 Grenade	—	430.0	430.0
	Total Mass	387.4	852.6	852.6

The modular payload system maintains center-of-gravity within acceptable limits for all mission configurations. The ISR configuration achieves optimal CG positioning with all components concentrated near the geometric center. Payload delivery and kamikaze configurations experience a 12 mm forward CG shift, which remains within the flight control system's compensation capability, ensuring stable flight characteristics across all operational modes.

3.6 Cost Analysis and Economic Feasibility

Tab. 4 presents the detailed cost analysis for COTS components based on current market pricing. The total component cost ranges from 415.15 USD to 433.66 USD depending on mission configuration requirements, with the variance primarily attributed to different airframe material requirements for payload mounting systems.

The production cost analysis considers development, tooling, and manufacturing expenses for small-batch production scenarios typical of tactical equipment procurement. Using the methodology from [18], the development support cost is estimated as:

$$C_{\text{dev}} = 257.75 \cdot W^{0.63} \cdot S^{1.3} \cdot (1+r)^{27} \tag{6}$$

where W is the MTOM in kg, S is the maximum speed in m/s, and r is the inflation rate. For the design parameters (W = 0.853 kg, S = 21 m/s, r = 0.0253), the development cost is approximately 30 060 USD.

Manufacturing analysis indicates that 100-unit production requires approximately 265 labor hours, resulting in a unit production cost of 774.26 USD including tooling and overhead. For comparison, the DJI Mavic 3 Pro costs 2 199 USD [19], with a payload dropping attachment adding 199 USD, totaling approximately 2 400 USD – representing a 68 % cost reduction versus commercial alternatives. The break-even analysis indicates profitability at production volumes exceeding 50 units, making the design economically viable even for limited military procurement quantities.

Tab. 4 Detailed cost analysis for COTS components

No.	Component	Manufacturer, Product	Price [USD]
1	Camera	RunCam, Eagle 3 Night Vision	69.99
2	Battery Pack	Tattu, R-Line 1550mAh 4S 130C	33.99
3	Communication/Telemetry	Matek, ELRS 2.4GHz Receiver R24S	19.99
4	Video Transmission	T-Motor, FT800	38.90
5	Flight Controller	T-Motor, F7 + F55A PRO II	137.90
6	Motors (4x)	T-Motor, F2004 1700KV	83.60
7	Propellers (4x)	DJI, Mini Pro Propellers	9.00
8	Airframe Material	Polycarbonate filament	21.80 to 39.29
		Total Component Cost	415.15 to 433.66

4 Performance Analysis

The performance evaluation methodology follows established rotorcraft analysis principles adapted for multirotor configurations [20]. Key performance metrics evaluated include maximum range (distance achievable at optimal cruise speed for each mission configuration), maximum endurance (flight time achievable at minimum power consumption speed), speed envelope (operational velocity range considering power limitations and mission requirements), and payload-range trade-offs (performance sensitivity to mission configuration variations).

4.1 Performance Analysis Methodology

All performance analyses were conducted using eCalc software [21] for multirotor design. To verify the software, the hovering performance was evaluated at ISR weight configuration (387.4 gram) using momentum theory [22].

Firstly, the nominal battery energy of Tattu R-line 1 550 mAh 4S 130C 14.8 V was modelled using Peukert's equation. From the generalized equation of Peukert's equation, for the capacity C = 1.55 Ah, the estimated current is i = 3.0 A to 3.5 A (see detail in [23] for comparison between equation and experimental data). The discharge time given by those values is in the range of (0.44–0.52) hour. By assuming all the variables constant, the available energy for this lithium polymer battery is approximately in the range of (22.79–22.94) Wh. The estimation is equal to the result produced by eCalc, that is 22.94 Wh.

By implementing the momentum theory over the control volume defined around the blade disk region, the power required to hover is equal to power done by the rotor and power required to overcome the profile drag of the quadcopter. In nondimensional form, the power coefficient C_p is given by [22].

$$C_\mathrm{p} = \frac{\kappa\sqrt{C_\mathrm{T}^3}}{\sqrt{2}} + \frac{\sigma C_{d_0}}{8} \tag{7}$$

where κ, σ, C_T, C_{d0} are induced power factor, rotor solidity (ratio between blade area and disk area), thrust coefficient, and profile drag coefficient, respectively. For the analysis, the κ is defined as 1.15 and the estimated σ for 2-blades quadrotor configuration is 0.092. The thrust coefficient defined by $C_\mathrm{T} = \frac{T}{\frac{1}{2}\rho A V_\mathrm{T}^2}$ gives the value of 0.0246 at 7 404 rev/min for each propeller. Note that the thrust T is equivalent to the weight of ISR configuration and V_T is the angular velocity of the rotor tip. By assuming the C_{d0} = 0.02 based on flat plate with the thickness-to-chord ratio of 0.37, the power coefficient is 0.00337.

Hence, the hovering power $P = 1/2\, \rho A V_\mathrm{T}^3 C_\mathrm{p}$ accounting for non-ideal induced loss is ~30.77 Watt. By considering the hovering thrust efficiency known as Figure of Merit (FM) that is given by:

$$FM = \frac{\dfrac{C_\mathrm{T}^{3/2}}{\sqrt{2}}}{\dfrac{\kappa C_\mathrm{T}^{3/2}}{\sqrt{2}} + \dfrac{\sigma C_{d_0}}{8}} \tag{8}$$

the actual mechanical power required for hovering is 37. 9 Watt. Here, the calculated FM is 0.81. By comparing the actual power of hovering, the momentum theory analysis gives a 0.9-Watt discrepancy that is larger than the value given by eCalc that is 37.0 Watt.

Assuming a moderate electric motor loss of 20 %, the electrical power required during hover is 47.37 W. Consequently, with ISR configuration, the total hovering time that can be achieved using this approach is around 29.1 minutes, while eCalc software is around 30.2 minutes. The discrepancy is understandable, considering eCalc software implement blade element theory that is more accurate than the approach using momentum theory. Based on this validation, further analysis is done using the eCalc software for multirotor configuration [19].

By evaluating the power loading (thrust/power in g/Watt), the flight efficiency during hover can be evaluated as mentioned in [24]. For quadcopter, the best hovering efficiency can be achieved if the configuration can generate a high-power loading, that is to reduce the required power. Improving blade design can increase the FM, thus reducing the hovering power [22].

4.2 Mission-Specific Performance Analysis

The ISR mission operates at the minimum system mass of 387.4 g, providing optimal power loading for extended operations. Maximum endurance of 30.0 min is achieved at hover or very low forward speeds (< 2 m/s), meeting the design goal specified in Tab. 2. Maximum range of 6 790 m occurs at the optimal cruise speed of 7 m/s – a 36 % improvement over the mandatory requirement of 5 000 m. Power consumption at optimal cruise is approximately 157 W, yielding a specific energy consumption of 1.73 Wh/km. The ISR configuration maintains endurance above 25 min for speeds up to 5 m/s, providing tactical flexibility for slow reconnaissance missions.

Both payload delivery and kamikaze missions operate at 852.6 g MTOM – a 120 % mass increase over the ISR configuration – which significantly impacts power loading and reduces both range and endurance. Maximum endurance is 9.5 min at low speeds (3 m/s), falling below the mandatory 15 min requirement. Maximum range of 2 989 m at 10 m/s cruise exceeds the mandatory 1 000 m requirement but represents a 56 % reduction versus ISR capability. Payload configurations show more rapid endurance degradation than ISR, dropping below 8 min at speeds exceeding 8 m/s, reflecting the higher wing loading. The optimal cruise speed increase from 7 m/s (ISR) to 10 m/s (payload) is consistent with this higher loading.

Fig. 7 illustrates these characteristic relationships across all mission configurations. The endurance curves exhibit relatively flat behavior at low speeds (0–5 m/s) where hovering power dominates, before decreasing rapidly beyond the minimum power speed due to parasitic drag losses. Range curves demonstrate the classic intermediate cruise speed optimum, with speeds above 12 m/s resulting in rapidly decreasing range for both configurations.

Maximum dash-speed evaluation confirms that both the ISR and payload configurations achieve 25.3 m/s at full power, exceeding the 21 m/s design target. However, this speed can only be sustained for approximately 1.5 min before battery depletion, limiting its tactical utility to rapid target engagement or evasive maneuvering scenarios.

4.3 Design Requirements Validation

Tab. 5 compares the calculated performance results against the design requirements established in Tab. 2. The analysis demonstrates that the design meets or exceeds mandatory requirements across most performance categories. The payload configuration endurance of 9.5 min falls below the mandatory requirement of 15 min. This deficiency indicates that either battery capacity must be increased or operational procedures must be modified to ensure mission success within the available flight time.

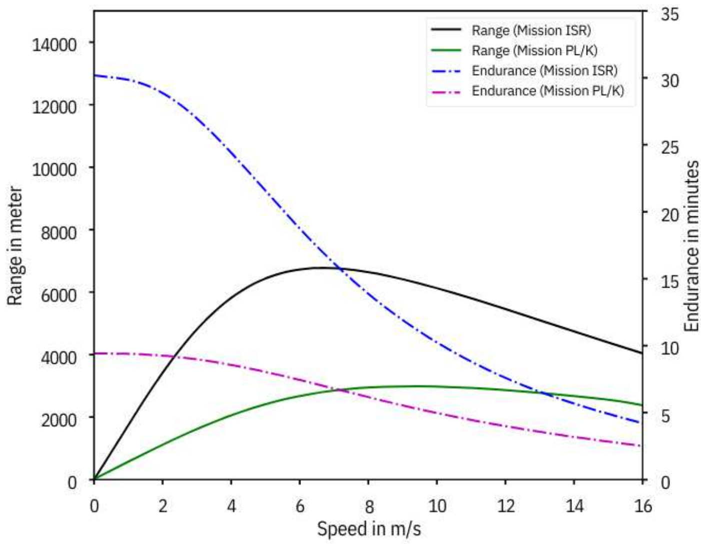

Fig. 7 Range and endurance performance envelope for all mission configurations. ISR mission (blue) demonstrates superior performance due to reduced mass, while payload delivery and kamikaze missions (red) show identical performance characteristics due to equivalent MTOM

Tab. 5 Performance validation against design requirements. Performance indicators: Δ exceeds design goal, ✓ meets mandatory requirement, x falls below mandatory requirement

Performance Metric	**Design Requirements**		**Achieved Performance**	
	Mandatory	**Goal**	**ISR**	**Payload**
Endurance at MTOM [min]	15	30	—	9.5 x
Endurance at MOEM [min]	30	60	30.0 ✓	—
Range at MTOM [m]	1 000	5 000	—	2 989 Δ
Range at MOEM [m]	5 000	10 000	6 790 ✓	-
Maximum Speed [m/s]	18	21	25.3 Δ	25.3 Δ

4.4 Comparative Analysis with Benchmark Platforms

Tab. 6 presents a comparative analysis of the designed quadcopter against the benchmark platforms (Viper40 and Drone40) across key performance metrics. The design achieves a 120 % increase in payload capacity, enabling compatibility with standard military ordnance, while endurance and range performance are reduced compared to commercial platforms, reflecting the fundamental trade-off between payload capacity and flight performance. The 68 % cost reduction provides significant economic advantages despite performance compromises, and maximum speed performance meets or exceeds commercial benchmarks across all configurations.

Tab. 6 Performance comparison with benchmark platforms. Performance indicators: Blue indicates improvement, Orange indicates trade-off relative to benchmark average

Performance Metric	Viper40	Drone40	This Design (Payload)	Improvement vs. Average
Payload Capacity [g]	200	190	430	+120 %
Endurance at MTOM [min]	25	30	9.5	−65 %
Range at MTOM [m]	1 000	20 000	2 989	−72 %
Maximum Speed [m/s]	18	20	25.3	+26 %
Unit Cost [USD]	~2 400		774	−68 %

4.5 Sensitivity Analysis and Design Optimization

Performance sensitivity to mass variations was evaluated to understand design robustness and optimization potential. A 5 %–10 % mass reduction through component optimization would improve endurance by approximately 8 %–16 % and range by 5 %–12 %, indicating moderate sensitivity to weight optimization efforts. Advanced lithium polymer batteries with 20 % higher energy density would increase range and endurance to 20 %, for payload missions, approaching the mandatory requirement. That is equivalent to 3 587 m in range and 11.4 min in endurance. This suggests that battery technology improvements represent the most effective path for performance enhancement.

Propeller optimization studies indicate that custom-designed propellers could increase FM, thus improve hovering efficiency by 8 %–12 %, translating to (1–2) min endurance improvements [22]. However, the additional development cost and complexity may not justify the modest performance gains for tactical applications requiring rapid deployment.

5 Conclusions and Future Work

5.1 Conclusions

This paper presented an open conceptual design of a multi-mission tactical quadcopter addressing critical payload limitations in existing commercial loitering munitions. Using COTS components, the design achieves (400–600) g payload capacity – a 120 % increase over commercial alternatives – enabling compatibility with standard military ordnance such as the Indonesian GT5-PEA2 defensive grenade (430 g). The modular design supports three mission profiles (ISR, payload delivery, and kamikaze operations) within a foldable configuration stowing within 180 mm, meeting infantry portability requirements.

Performance analysis confirms the ISR configuration meets all design goals, achieving 30 min endurance and 6 790 m range at 387.4 g operating weight. The payload configuration achieves 2 989 m range, exceeding the 1 000 m mandatory requirement, though endurance of 9.5 min falls below the 15 min mandatory threshold – a fundamental trade-off inherent to small multirotor systems carrying significant payload fractions. Economic analysis yields a unit production cost of 774 USD for 100-unit runs, representing a 68 % reduction versus approximately 2 400 USD commercial alternatives. The publicly available CAD documentation and design methodology facilitate collaborative development and rapid adaptation by organizations with limited R&D resources.

5.2 Future Work

Several directions merit further investigation. Battery technology represents the most impactful optimization path, as a 20 % increase in energy density would bring payload endurance to approximately 11.4 min, approaching the mandatory requirement. Custom propeller design could improve hovering efficiency by 8 %–12 %, yielding (1-2) min additional endurance. Beyond propulsion improvements, integration of autonomous navigation and target recognition capabilities would reduce operator workload and improve mission effectiveness. Swarm coordination protocols and expanded payload options – including sensors, communication relays, and non-lethal systems – would further extend operational utility. Environmental hardening for high-altitude and adverse weather operation, along with comprehensive release mechanism validation under combat conditions, are prerequisites for operational deployment.

References

[1] TELLER, J. Regulating Urban Densification: What Factors Should Be Used? *Buildings and Cities*, 2021, **2**(1), pp. 302-317. DOI 10.5334/bc.123.

[2] SPENCER, J. and J. GEROUX. *Defending the City: An Overview of Defensive Tactics from the Modern History of Urban Warfare* [online]. 2022 [viewed 2026-03-08]. Available from: https://mwi.westpoint.edu/defending-the-city-an-overview-of-defensive-tactics-from-the-modern-history-of-urban-warfare/

[3] GLENN, R.W. *Combat in Hell: A Consideration of Constrained Urban Warfare* [online]. 2002 [viewed 2026-03-08]. Available from: https://www.rand.org/pubs/monograph_reports/MR780.html

[4] VAUTRAVERS, A. Military Operations in Urban Areas. *International Review of the Red Cross*, 2010, **92**(878), pp. 437-452. DOI 10.1017/S1816383110000366.

[5] *Military Operations on Urbanized Terrain (MOUT)*. 2018 [online]. [viewed 2026-03-08]. Available from: https://www.marines.mil/News/Publications/MCPEL/Electronic-Library-Display/Article/900535/mcrp-12-10b1/

[6] VALAVANIS, K.P. and G.J. VACHTSEVANOS. *Handbook of Unmanned Aerial Vehicles*. Dordrecht: Springer, 2014. ISBN 90-481-9706-6.

[7] BODE, I. and T.F.A. WATTS. *Loitering Munitions and Unpredictability: Autonomy in Weapon Systems and Challenges to Human Control* [online]. 2023 [viewed 2026-03-08]. DOI 10.5281/zenodo.8379571.

[8] VOSKUIJL, M. Performance Analysis and Design of Loitering Munitions: A Comprehensive Technical Survey of Recent Developments. *Defence Technology*, 2022, **18**(3), pp. 325-343. DOI 10.1016/j.dt.2021.08.010.

[9] ZHUGAN, O. and M.O. DEGTYAREV. Version of Loitering Munitions Classification Based on the State-of-the-Art and Trends Analysis. *Space Science and Technology*, 2024, **30**(3), pp. 31-39. DOI 10.15407/knit2024.03.031.

[10] *FM 21-18 Foot Marches* [online]. 1990 [viewed 2026-03-08]. Available from: https://archive.org/details/milmanual-fm-21-18-foot-marches

[11] LOVERRO, K.L., L. HASSELQUIST and C.L. LEWIS. Females and Males Use Different Hip and Knee Mechanics in Response to Symmetric Military-Relevant Loads. *Journal of Biomechanics*, 2019, **95**, 109280. DOI 10.1016/j.jbiomech.2019.07.024.

[12] KNAPIK, J.J., K.L. REYNOLDS and E. HARMAN. Soldier Load Carriage: Historical, Physiological, Biomechanical, and Medical Aspects. *Military Medicine*, 2004, **169**(1), pp. 45-56. DOI 10.7205/milmed.169.1.45.

[13] *GT5-PEA2 Defensive Hand Grenade* [online]. [viewed 2026-03-08]. Available from: https://web.archive.org/web/20260207035529/https:// pindad.com/gt5-pea2

[14] VU, N.A., D.K. DANG and T.L. DINH. Electric Propulsion System Sizing Methodology for an Agriculture Multicopter. *Aerospace Science and Technology*, 2019, **90**, pp. 314-326. DOI 10.1016/j.ast.2019.04.044.

[15] BICZYSKI, M., R. SEHAB, J.F. WHIDBORNE, G. KREBS and P. LUK. Multirotor Sizing Methodology with Flight Time Estimation. *Journal of Advanced Transportation*, 2020, **2020**, 9689604. DOI 10.1155/2020/9689604.

[16] AUSTIN, R. *Unmanned Aircraft Systems: UAVs Design, Development and Deployment*. Chichester: Wiley, 2010. ISBN 0-470-05819-6.

[17] GAO, W., et al. The Status, Challenges, and Future of Additive Manufacturing in Engineering. *Computer-Aided Design*, 2015, **69**, pp. 65-89. DOI 10.1016/j.cad.2015.04.001.

[18] NICOLAI, L.M. and G.E. CARICHNER. *Fundamentals of Aircraft and Airship Design: Volume I – Aircraft Design*. Reston: American Institute of Aeronautics and Astronautics, 2010. ISBN 1-60086-753-7.

[19] *Consumer Drone Comparison* [online]. 2025 [viewed 2026-03-08]. Available from: https://www.dji.com/products/comparison-consumer-drones

[20] SEDDON, J.M. and S. NEWMAN. *Basic Helicopter Aerodynamics*. 3rd ed. Chichester: Wiley, 2011. ISBN 0-470-66537-8.

[21] *eCalc – xcopterCalc – the Most Reliable Multicopter Calculator on the Web* [online]. [viewed 2026-03-08]. Available from: https://www.ecalc.ch/xcoptercalc.php

[22] LEISHMAN, J.G. *Principles of Helicopter Aerodynamics*. 2nd ed. Cambridge: Cambridge University Press, 2006. ISBN 978-0-521-85860-1.

[23] GALUSHKIN, N., N. YAZVINSKAYA and D. GALUSHKIN. A Critical Review of Using the Peukert Equation and its Generalizations for Lithium-Ion Cells. *Journal of the Electrochemical Society*, 2020, **167**(12), 120516. DOI 10.1149/1945-7111/abad69.

[24] CAI, X., S.K.H. WIN and S. FOONG. QuadRotary: Design and Control of In-Flight Transition Between Quadcopter and Rotary-Wing. *IEEE/ASME Transactions on Mechatronics*, 2025, **30**(6), pp. 5376-5386. DOI 10.1109/TMECH.2025.3556021.